

# **Effect of Post-HALT Annealing on Leakage Currents in Solid Tantalum Capacitors**

Alexander Teverovsky

Dell Perot Systems

GSFC/NASA Code 562, Greenbelt, MD 20771  
Alexander.A.Teverovsky@nasa.gov

## **Abstract**

Degradation of leakage currents is often observed during life testing of tantalum capacitors and is sometimes attributed to the field-induced crystallization in amorphous anodic tantalum pentoxide dielectrics. However, degradation of leakage currents and the possibility of annealing of degraded capacitors have not been investigated yet. In this work the effect of annealing after highly accelerated life testing (HALT) on leakage currents in various types of solid tantalum capacitors was analyzed. Variations of leakage currents with time during annealing at temperatures from 125 °C to 180 °C, thermally stimulated depolarization (TSD) currents, and I-V characteristics were measured to understand the conduction mechanism and the reason for current degradation. Annealing resulted in a gradual decrease of leakage currents and restored their initial values. Repeat HALT after annealing resulted in reproducible degradation of leakage currents. The observed results are explained based on ionic charge instability (drift/diffusion of oxygen vacancies) in the tantalum pentoxide dielectrics using a modified Schottky conduction mechanism.

## **Introduction.**

Failures of tantalum capacitors under steady-state conditions might occur as a sudden increase of a LC without noticeable degradation and are often attributed to the field-induced crystallization in amorphous Ta<sub>2</sub>O<sub>5</sub> dielectrics [1-2]. The field-induced crystallization model assumes that tantalum oxide crystals are growing with time of operation under the amorphous anodic oxide and eventually disrupt the dielectric layer, causing a breakdown. Until the moment of disruption, the integrity of the dielectric is not compromised and no changes in leakage currents are observed. It is assumed that the rate of crystallization increases with increasing thickness of the anodic oxide [2] and high-voltage capacitors should be more vulnerable to this type of failure. Tantalum oxide crystals and fractured dielectric layers were often observed on the surface of wet and solid tantalum capacitors after high-voltage electrical stresses. However, Ikonopisov [3] suggested that the formation of crystals is a result of breakdowns, rather than their prime cause.

Laleko and co-workers [4-5] studied extensively Ta-Ta<sub>2</sub>O<sub>5</sub>-MnO<sub>2</sub> structures with anodic dielectrics and detected a significant increase of LC with time at high electric fields ( $> 3 \times 10^8$  V/m). It was concluded that despite of its negligible value, ionic currents in the dielectric change the spectrum of localized electronic states in the forbidden band of Ta<sub>2</sub>O<sub>5</sub>, activate the conductivity of the oxide, and cause irreversible changes in the electrical properties of the system. Resistance degradation in TiN/Ta<sub>2</sub>O<sub>5</sub>/TiN MIM (Metal-Insulator-Metal) structures with deposited amorphous Ta<sub>2</sub>O<sub>5</sub> dielectrics was also observed by Manceau et al. [6-7]. The rate of degradation accelerated exponentially as the temperature increased from room to 200 °C. The results were explained by migration of oxygen vacancies that initially are accumulated near the electrodes. Similar to the mechanism suggested by Laleko, it was assumed that the conductivity of oxide depends on the concentration of oxygen vacancies and increases as vacancies are migrating from electrodes towards the bulk of the oxide.

Degradation of LC during life testing of solid tantalum capacitors has been reported in several publications [8-10]. Zednicek and co-authors [11] presented data indicating a substantial, up to 3 orders of magnitude, increase in LC in

one abnormal batch of 33 uF/35 V capacitors during 125 °C life test at 0.66VR. Although less significant, increasing LCs (10 to 15 times) were also observed even in a normal, reference lot of parts. Two other lots of 150 uF/16 V capacitors increased LCs at 125 °C more than 3 orders of magnitude approaching the specified limit after 2000 hours of testing. However, failure analysis indicated the presence of crystals in both, normal and abnormal lots of 33 uF/35 V capacitors, and no signs of field crystallization were found in 150 uF/16 V batches with abnormally high LCs. The conclusion of this work was that field crystallization may not be the only or even the main driving process responsible for failures.

Obviously, there is a need for more data related to current degradation in chip tantalum capacitors, factors affecting this degradation, and analysis of possible mechanisms. In this work, LCs in various types of solid tantalum capacitors degraded during highly accelerated life test (HALT) conditions at temperatures from room up to 170 °C and voltages up to two times the rated voltage were annealed at different temperatures. Variations of LCs with time during annealing, thermally stimulated depolarization currents, and I-V characteristics were measured to understand the conduction mechanism and the reason for current degradation. The observed kinetics of current variation is explained based on charge instability in the tantalum pentoxide dielectrics using a modified Schottky conduction mechanism.

### **Experiment.**

To reveal common features in current degradation in chip tantalum capacitors different types of commercial and military-grade parts manufactured by three vendors were used in this study. The values of capacitance varied from 4.7 uF to 220 uF and the values of rated voltages, VR, from 6 V to 63 V.

Leakage currents in the parts were monitored during highly accelerated life testing (HALT) and annealing using a PC-based data acquisition system. A typical duration of HALT was 100 hrs, while temperature and voltage varied from 105 °C to 170 °C and from 0.8VR to 2VR. During annealing the parts were shorted, and leakage currents were measured periodically by applying a certain testing voltage, that was typically lower than the stress voltage, for a relatively short period of time (typically for 5 min).

I-V characteristics of capacitors were measured before, after HALT, and after annealing. To reduce errors related to absorption currents, the current decay after voltage application was recorded, and the readings of LCs were taken after 1000 seconds of electrification.

Thermally stimulated depolarization (TSD) currents were measured to better understand the nature of charge relaxation processes in tantalum capacitors and to estimate their activation energies. The samples were heated typically from -10 °C to 180 °C at a constant rate of 3 °C /min while their depolarization currents were measured. TSD measurements followed immediately the stress testing (or thermally stimulated polarization TSP) cycle during which the part was heated to 170 °C and cooled down to -20 °C at a rate of 3 °C /min under a certain polarization voltage. Analysis of the TSD spectrums was carried out using a first order model originally developed to explain thermoluminescent peaks in dielectrics [12]. This model allows for calculation of the TSD current for a system that is heating up with a rate  $\beta$  starting from temperature  $T_0$ :

$$i(T) = qsn_0 \exp\left[-W/kT - \left(\frac{s}{\beta}\right) \int_{T_0}^T \exp(-W/kT) dT\right], \quad (1)$$

where  $q$  is the electron charge,  $n_0$  is the initial concentration of carriers on the traps,  $W$  is the activation energy, and  $s$  is the trap escape frequency factor. The best fit approximation technique was used to estimate activation energies of relaxation processes,  $W$ .

### **Results.**

Capacitors with currents degraded during HALT (typically 100 hours at 130 °C to 155 °C, and rated voltage) were annealed at temperatures in the range from 125 °C to 160 °C for periods varying from 40 hours to 120 hours, while their currents were measured periodically at a certain testing voltage. Results of these measurements for 15 uF/10 V and 47 uF/20 V capacitors are shown in Figure 1. Note, that the current decrease with time can be linearized when

logarithm of the current is plotted against the square root of bake time. This suggests an exponential dependence of current on time that can be expressed as:

$$J = B \times \exp(-\alpha t^{0.5}), \quad (2)$$

where  $B$  is a constant, and  $\alpha$  is the rate of current recovery.

Note that in  $\log(J) - t^{0.5}$  coordinates the lines corresponding to samples having different current levels after HALT have approximately the same slopes during annealing.

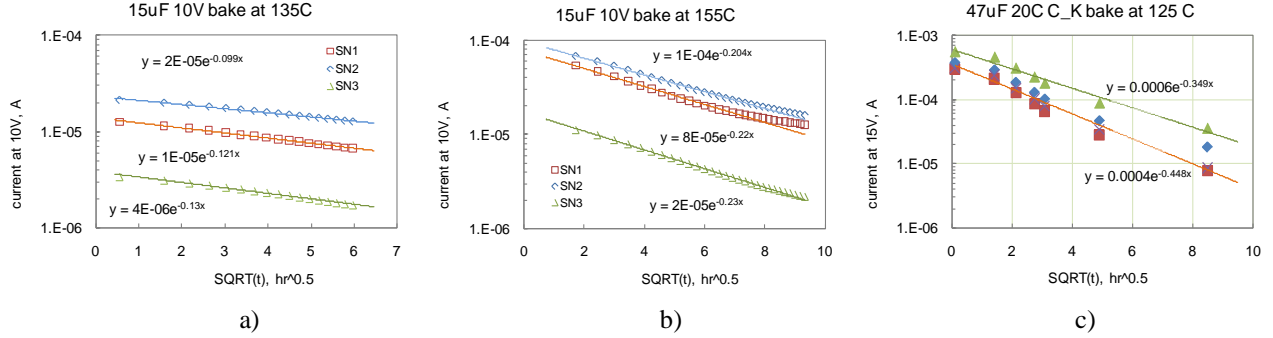


**Figure 1.** Effect of post-HALT annealing at 135 °C (a) and 155 °C (b) for 15 uF/10 V capacitors and at 125 °C for 47 uF/20 V capacitors (c).

Results of annealing of three different types of high-voltage capacitors at three temperatures are shown in Figure 2. In all cases the decrease of currents follows Eq.(3), and the rate of recovery increases with temperature. Annealing at 160 °C for 120 hours and at 180 °C for 36 hours restored almost completely initial current levels in the parts. However, annealing at 140 °C for 100 hours resulted in partial recovery only.

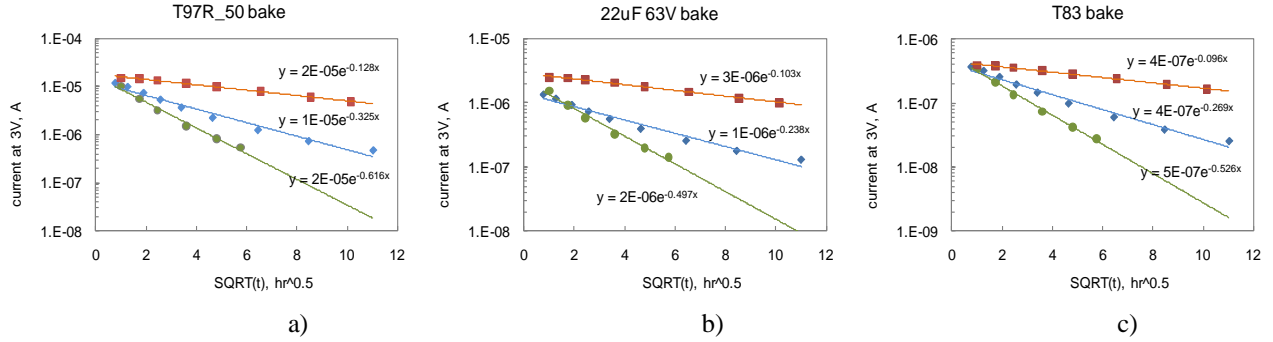


**Figure 2.** Effect of post-HALT annealing at three temperatures for 22 uF/50 V (a), 22 uF/63 V (b), and 4.7 uF/50 V (c) capacitors.

Five samples of six different types of high-voltage capacitors rated to 50 V and 63 V were stressed by 100-hour HALT at 155 °C/50 V initially, then the second time after bake at 160 °C for 120 hours, and for the third time after bake II at 180 °C for 36 hours. Results of repeat HALT for two part types are shown in Figures 3 and 4 and indicate reproducibility of the current degradation after bake. Note, that one of the samples in Figure 4 failed after 48 hours of the stress during initial HALT due to the current increase to more than 10 mA. However, even this failed sample recovered after the bake and then manifested the same behavior failing after 21 hours during HALT-2 and after 26 hours during HALT-3.

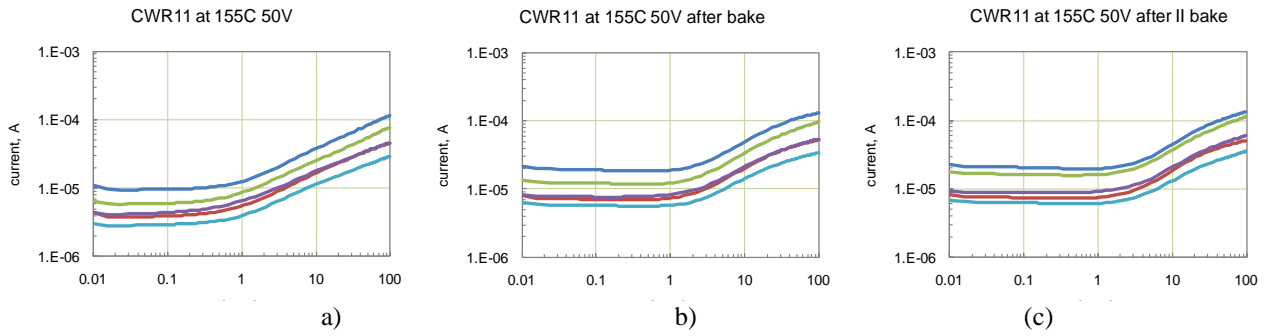


**Figure3.** Current degradation in five 4.7uF/50V CWR11-style capacitors at 155 °C 50V. Initial test (a) after annealing at 160 °C for 100 hours (b), and after annealing at 180 °C for 100 hours (c).

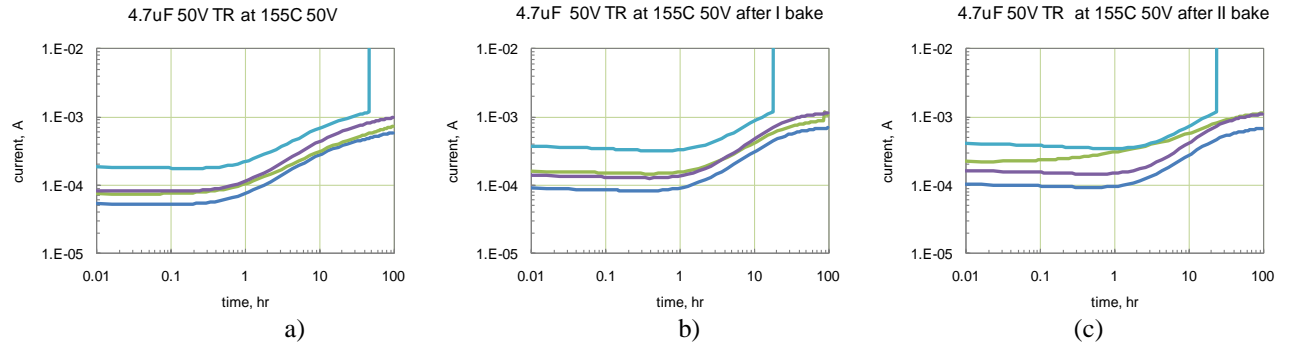


**Figure 4.** Current degradation in four 22 uF/50V capacitors at 155 °C 50V. Initial test (a) after annealing at 160 °C for 100 hours (b), and after annealing at 180 °C for 100 hours (c).

## Discussion.

A model of current degradation described below is based on the notions developed back in 1970s by Klein and Jaeger [13-14] who explained an increase in conductivity of anodic tantalum oxide films with time under high electric field as a result of lowering of the emission barrier due to ionic (oxygen vacancies) interface polarization. According to their model, the barrier decreases with time linearly with a rate that increases with the applied voltage. Note, that similar qualitative models have been used also to describe ageing processes (degradation of leakage currents with time under bias) in rutile (TiO<sub>2</sub>) ceramics [15], zinc oxide varistors [16], and ceramic capacitors [17].

To explain the results of current degradation obtained in this work we assume that a large concentration of oxygen vacancies exists initially at the Ta/Ta<sub>2</sub>O<sub>5</sub> interface. At high temperature and high electric fields positively charged oxygen vacancies are drifting towards the cathode, and due to blocking characteristics of the MnO<sub>2</sub>/Ta<sub>2</sub>O<sub>5</sub> contact, they are piling up at the cathode. This increases local electrical field and decreases the height of the cathode barrier thus increasing electron emission to the oxide. Due to a limited quantity of the vacancies and electron trapping that neutralizes positively charged vacancies, the degradation process stabilizes with time resulting in a decrease of the rate of degradation. Annealing of the capacitors after HAST redistributes vacancies back to the bulk of Ta<sub>2</sub>O<sub>5</sub> film thus restoring the initial level of the current.

### Effect of charges in Ta<sub>2</sub>O<sub>5</sub> on I-V characteristics.

Multiple studies have shown that the electron transport in Ta<sub>2</sub>O<sub>5</sub> dielectrics is due either to a bulk-limited Poole-Frenkel conduction or to surface-barrier-limited Schottky mechanisms [18-21]. It is assumed that different conduction mechanisms can prevail in different ranges of voltage and temperature, and can vary depending on the treatment of the oxide (e.g. annealing conditions) [22]. A detailed analysis of different conduction mechanisms in Ta<sub>2</sub>O<sub>5</sub> dielectrics was performed by Novkovski and Atanassova [23]. Anodic tantalum oxide films have a

disordered structure and a substantial amount of electron traps, up to  $10^{19} \text{ cm}^{-3}$ , so electron transport through the oxide is commonly described as Poole-Frenkel conduction. This conduction limits the electron flow for the metal/Ta<sub>2</sub>O<sub>5</sub> systems for which the Fermi level of the metal is close or above the level of electron traps. In this case electrons can easily penetrate to the traps (e.g. via tunneling) and their transport is controlled by Poole-Frenkel mechanism. However, for electrodes having large work function or electron affinity, the position of Fermi level can be much below the level of traps, and the current will be limited by the Schottky emission. This is likely the case when MnO<sub>2</sub> is used as a cathode material because of a high affinity to electrons of manganese oxide, ~ 5.3 eV, [24]. Estimations made in this work showed that the barrier height at the MnO<sub>2</sub>/Ta<sub>2</sub>O<sub>5</sub> interface is ~ 0.62 eV.

Although discrimination of the conduction mechanisms for tantalum capacitors having large surface areas and non-uniform thickness of the dielectric remains a challenge, our experimental results can be explained in terms of the Schottky model. The major justification for this model is rectifying I-V characteristics of tantalum capacitors and the effect of electrodes observed in MOM structures with Ta<sub>2</sub>O<sub>5</sub> dielectrics by different authors [13, 25-26]. Increased leakage currents in solid tantalum capacitors with polymer cathodes compared to regular parts having MnO<sub>2</sub> cathodes were also explained by the difference in the energy barriers at the cathode/Ta<sub>2</sub>O<sub>5</sub> interfaces that controls emission of electrons in the dielectric [27].

According to Schottky theory, the electron flow in the metal-dielectric system is limited by a surface energy barrier,  $q\Phi_B$ , that can be determined as a difference in energy between the Fermi level of the cathode material and the bottom of the conduction band of the dielectric. The current density corresponding to this flow,  $J$ , is an exponential function of the electric field in the dielectric,  $E^{1/2}$ :

$$J_{Sch} = C_{RD} T^2 \exp\left(-\frac{q\Phi_B}{kT}\right) \exp\left[\frac{1}{kT} \left(\frac{q^3 E}{4\pi\epsilon\epsilon_0}\right)^{1/2}\right], \quad (3)$$

where  $C_{RD} = 1.2E6 \text{ A/m}^2 \text{ K}^2$  is the Richardson-Dushman constant,  $q$  is the charge of electron,  $k$  is the Boltzmann constant,  $T$  is the absolute temperature;  $\epsilon_0$  is the permittivity of the free space, and  $\epsilon \sim 5$  is the high-frequency dielectric constant for Ta<sub>2</sub>O<sub>5</sub>.

This equation can accurately predict field emission in metal-vacuum systems, but its application to metal-dielectric systems results in anomalously high currents. Aries [28] explained this by an assumption of the presence of not only a surface barrier in the dielectric, but also a barrier at the surface of the cathode material. The applied field does not affect substantially the cathode barrier, but influences the metal-oxide barrier and causes current variations as predicted by Eq.(4). To penetrate to the dielectric, electrons have to tunnel through the cathode barrier, so their flow to the dielectric is reduced drastically. In this case Eq.(4) can be used to describe metal-dielectric systems, but instead of the Richardson-Dushman constant, an empirical parameter  $C_1$  should be used.

The Schottky barrier lowering can be derived based on relatively simple electrostatic calculations of distributions of electrostatic potential at the interface caused by external electrical field,  $E$ , and a field created by the interaction between the electron leaving the metal and the induced positive charge. This interaction of fields results in reduction of the barrier  $\Phi_B$  with external field so the effective barrier height is:

$$\Phi = \Phi_B - \sqrt{\frac{q^3 E}{4\pi\epsilon\epsilon_0}}, \quad (4)$$

Charges inside Ta<sub>2</sub>O<sub>5</sub> dielectrics of tantalum capacitors will create additional electric field  $E_c$  that will also affect the barrier height, and Eq.(5) can be presented as:

$$\Phi = \Phi_B - \sqrt{\frac{q^3 (V/d + E_c)}{4\pi\epsilon\epsilon_0}}, \quad (5)$$

where  $V$  is the applied voltage, and  $d$  is the thickness of the dielectric.

To assess  $E_c$ , we can assume that the charge in a Ta<sub>2</sub>O<sub>5</sub> film is placed at a distance  $x$  from the cathode and have a sheet density of  $Q_s$ . With this simplification the charge-induced field at the cathode can be expressed as:

$$E_c = \frac{Q_s}{\epsilon \epsilon_0} \left( 1 - \frac{x}{d} \right) \quad (6)$$

Substitution of (6) and (7) in (4) yields an expression for I-V characteristics of a tantalum pentoxide dielectric that reflects the effect of charges in the oxide:

$$J = C_1 T^2 \exp\left(-\frac{q\Phi_B}{kT}\right) \exp\left[\frac{\beta_s}{kT} \left(\frac{V}{d} + \frac{Q_s}{\epsilon \epsilon_0} \left(1 - \frac{x}{d}\right)\right)^{0.5}\right], \quad (7)$$

where  $\beta_s = \left(\frac{q^3}{4\pi\epsilon\epsilon_0}\right)$  is the Schottky constant.

Several studies have indicated that the specific of anodic oxide films on tantalum is the presence of large concentration of positively charged oxygen vacancies located at the Ta/Ta<sub>2</sub>O<sub>5</sub> interface [2, 6, 25]. Based on Eq.(7), charges located at the anode interface ( $x = d$ ) will not affect leakage currents at normal operation polarity (negative potential is at manganese cathode). During operation, a voltage applied to a capacitor will cause migration of oxygen vacancies in Ta<sub>2</sub>O<sub>5</sub> dielectric from anode to cathode thus increasing  $E_c$  and LC.

#### Effect of annealing.

During annealing at short circuit conditions, the ions in Ta<sub>2</sub>O<sub>5</sub> dielectric will diffuse from the cathode thus reducing the effective electrical field at the cathode interface. Let us assume that the centroid of the charge is moving with time as the length of diffusion, so  $x \approx D^{0.5} t^{0.5}$ , where  $D$  is the diffusion coefficient. Obviously, this approach neglects the charge-induced electric field in the oxide and distribution of charges in the bulk of oxide, and can be used for rough estimations only.

During initial stages of annealing, when  $x$  is small compared to the thickness of the oxide,  $d$ , the following approximation can be made:

$$\left(1 - \frac{x}{d}\right)^{0.5} \approx 1 - \frac{D^{0.5}}{2d} t^{0.5}$$

In this case Eq.(7) can be presented in the form of Eq.(3) where the rate of recovery,  $\alpha$ , can be expressed as:

$$\alpha = \frac{\beta_s}{kT} \left(\frac{Q_s}{\epsilon \epsilon_0}\right)^{0.5} \frac{D^{0.5}}{2d} \quad (8)$$

Parameter  $\alpha$  can be calculated using kinetics of the current recovery during annealing by plotting logarithm of the current versus square root of time. Using this equation and estimations for  $Q_s$  (from 0.005 to 0.03 C/m<sup>2</sup>), the diffusion coefficients of ions,  $D$ , can be calculated at different temperatures. The values of  $D$  obtained as a result of these estimations for five part types at three annealing temperatures are plotted in Arrhenius coordinates in Figure 5.

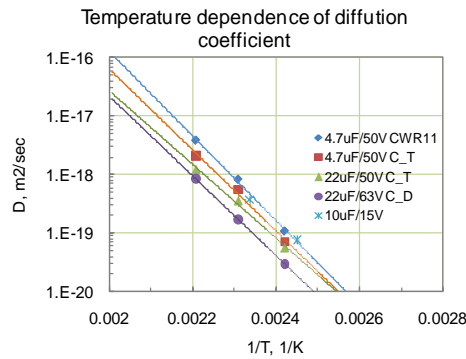


**Figure 5.** Temperature dependencies of diffusion coefficients of oxygen vacancies for different tantalum capacitors.

From  $D(T)$  dependencies the activation energy of diffusion process is derived to be in the range from 1.1 eV to 1.3 eV, which is close to the activation energy reported for oxygen vacancies in ceramic materials by Zafar et al. [29] (1 to 1.1 eV) and by Liu and Randall [30] ( $1.1 \pm 0.09$  eV).

#### Thermally stimulated depolarization currents.

Results of measurements of thermally stimulated depolarization (TSD) currents for three part types are shown in Figure 6. These measurements followed the thermally stimulated polarization (TSP) at different voltages varying from rated to twice rated voltage for low-voltage parts, and from  $0.4*VR$  to  $1.2*VR$  for parts rated to 50V. The spectrums of TSD currents indicate the presence of three peaks (peaks A, B, and C for future references). Peak A has a maximum at temperatures below 25 °C and was likely related to a relatively fast electron trapping processes. Peak B has maximum at approximately 75 °C and was clearly observed for all part types. Peak C has a maximum at temperatures exceeding  $\sim 150$  °C and due to a limited temperature range during TSD measurements was observed in a few cases only. However, increasing TSD currents at  $T > \sim 125$  °C indicate the presence of this peak in all parts.

The amplitudes of all three peaks are changing with polarization conditions. At relatively low voltages, below  $1.5*VR$ , peak B is linearly increasing with voltage, but its amplitude stabilizes at higher voltages. Peak C does not saturate at least up to  $2*VR$ , and is apparently shifting towards lower temperatures as the voltage during TSP increases.

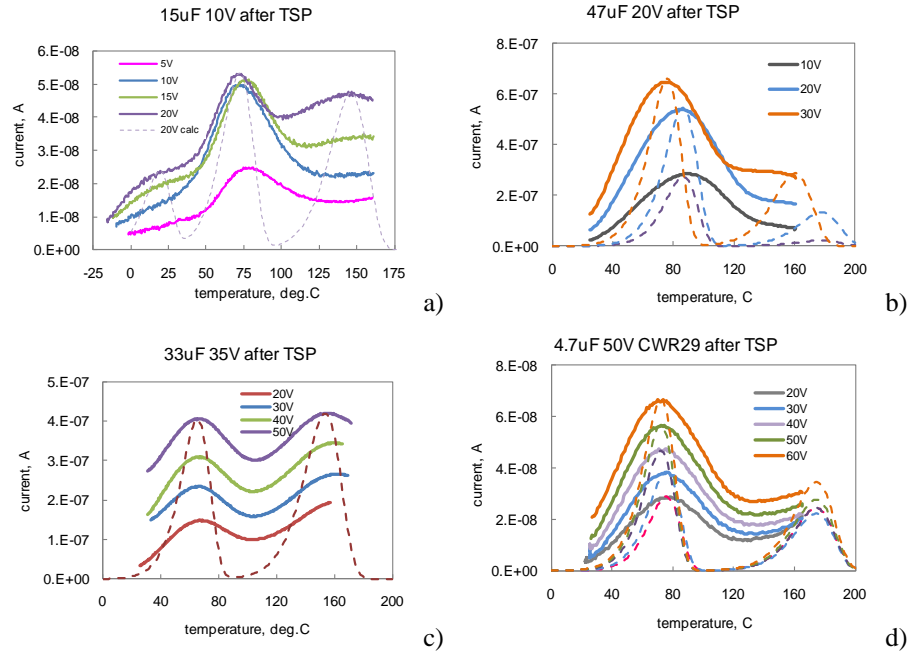


**Figure 6.** Evolution of thermally stimulated depolarization (TSD) current spectrums for 15uF/10V (a), 47uF/20V (b), 33uF/35V (c), and 4.7uF/50V (d) capacitors after thermally stimulated polarization (TSP) cycles at different voltages. Dashed lines are calculations per Eq.(1).

The effect of HALT stress conditions on TSD spectrums is presented for three high-voltage parts in Figure 7. For these parts only peaks B and C were revealed. Both peaks increased with voltage up to  $1.3*VR$ . Peak B depends mostly on polarization voltage, and does not change much with temperature and duration of the stress, whereas peak C increases with time under the stress and apparently shifts towards lower temperatures. For example, for 22 uF/63 V capacitors polarized at 50V and 155 °C, an increase of duration from  $\sim 0.5$  hr to 30 hrs increases TSD currents at 175 °C,  $I_{175}$ , by  $\sim 50\%$ , from  $1.2E-7$  A to  $\sim 1.8E-7$  A. For 4.7 uF/50 V C\_R type capacitors increasing polarization time from 1 hr to 15 hr at 145 °C/50 V HALT resulted in increasing of  $I_{175}$  from  $1.3E-8$  A to  $1.8E-8$  A.

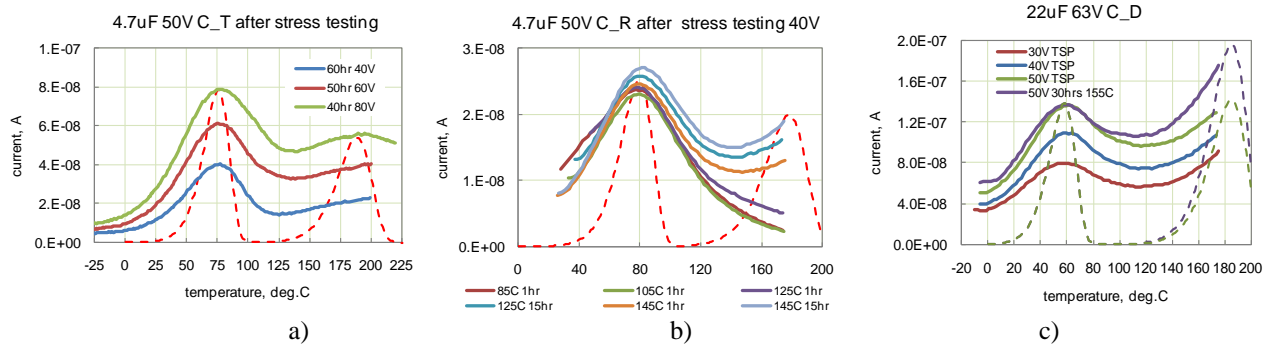


**Figure 7.** Thermally stimulated depolarization (TSD) current spectra for 4.7uF/50V, type C\_T (a), 4.7uF/50V, type C\_R (b), and 22uF/63V (c) capacitors after different HALT conditions. Dashed lines are calculations per Eq.(1).

Using the best-fit approximation, the energy levels associated with different peaks were calculated (see dashed lines in Figure 6 and 7) and results of these calculations are displayed in Table 1. Peak B is identical for all parts and corresponds to activation energy in the range from 0.91 eV to 0.96 eV. Most likely, this peak corresponds to electron trapping into deep electron states in the band gap of Ta<sub>2</sub>O<sub>5</sub> oxide and is related to intrinsic defects of the anodic film.

Oxygen vacancies are double donors and can create deep electron states in the band gap of tantalum pentoxide dielectrics. Lau et al. [31-32] studied Ta<sub>2</sub>O<sub>5</sub> films formed on silicon using a chemical vapor deposition (CVD) technique and estimated that the first ionized state of the oxygen vacancy is 0.8 eV below the conductive band of the dielectric. This corresponds to the theoretical calculations by Sawada and Kawakami [33]. Different ionization levels of oxygen vacancies and formation of complexes with contaminations such as Si and C can result in a large range of energy states in the band gap of tantalum pentoxide dielectric [34]. It is possible that in our case peak B also corresponds to electron trapping on local states related to oxygen vacancies in the dielectric.

**Table 1.** Activation energies (eV) of relaxation processes

Parameter	10uF/15V CWR11	47uF/20V	33uF/35V	4.7uF/50V CWR	4.7uF/50V C_T	22uF/50V	22uF/63V
Peak A	0.8						
Peak B	0.95	0.96	0.93	0.95	0.96	0.96	0.91
Peak C	1.16	>1.2	1.19	>1.24	1.28	>1.27	>1.27
Charge peak C, C	3.7E-5	>2.2E-4	3E-4	>2.2E-5	4.4E-5	>1.5E-5	>1.3E-4

Estimations showed that peak C corresponds to relaxation processes with activation energies varying from 1.16 eV to 1.28 eV and is likely due to a transport of positively charged oxygen vacancies in the oxide. The energy levels of this peak match to the activation energies of diffusion coefficients of the movable charges estimated based on current degradation under HALT and their recovery during annealing. Also, the value of the charge, associated with peak C and calculated as an integral of TSD currents varies in the range from 3.7E-5 C to 3E-4 C that is close to the total charge values,  $Q_t$ , calculated based on modeling of the current degradation during HALT.

## Conclusion.

1. HALT-induced degradation is reversible and leakage currents are gradually decreasing with time during annealing. The recovery is near to completion after annealing at 160 °C for ~ 120 hrs. The activation energy of annealing is in the range from 1.1 eV to 1.3 eV.
2. Repeat HALT after the parts have been annealed resulted in degradation that is similar to the one observed initially thus indicating reproducibility of the degradation process.

3. Degradation of leakage currents with time during HALT and their recovery during annealing are explained based on ionic charge instability in the tantalum pentoxide dielectrics using a modified Schottky conduction mechanism. The ionic drift results in accumulation of positive charges at the cathode interface that enhances injection of electrons and increases leakage currents and diffusion during annealing redistributes ions inside the oxide, reduces the effective charge at the interface, decreases leakage current, and explains reversibility of current degradation.
4. All capacitors had spectrums of TSD current with two characteristic peaks corresponding to relaxation processes with activation energies of  $0.93 \pm 0.02$  eV and to more than 1.1 eV. The first peak reflects electron trapping at the energy states located deep in the band gap of the oxide, and the second is due to transport processes (drift/diffusion) of positively charged oxygen vacancies.

### Acknowledgment.

This work was sponsored by the NASA Electronic Parts and Packaging (NEPP) Program. The author is thankful to the Program Managers, Michael Sampson and Ken LaBel, for their support and encouragement, and appreciates the help of Manufacturers of tantalum capacitors for providing samples for this study.

### References.

- [1] B. Goudswaard and F. J. J. Driesens, "Failure mechanism of solid tantalum capacitors," *Electrocomponent Science and Technology*, vol. 3, pp. 171-179, 1976.
- [2] T. Tripp and Y. Freeman, *Major Degradation Mechanisms in Tantalum and Niobium Based Capacitors*: Components Technology Institute Inc., 2008.
- [3] S. Ikonopisov, "Theory of electrical breakdown during formation of barrier anodic films," *Electrochimica Acta*, vol. 22, pp. 1017-1082, 1977.
- [4] V. A. Laleko, L. L. Odinets, and G. B. Stefanovich, "Ionic current and kinetics of "activation" of the conductivity (degradation) of anodic oxide films on tantalum in strong electric fields," *Soviet Electrochemistry*, vol. 18, pp. 743-746, 1982.
- [5] V. A. Laleko, V. P. Malinenko, and G. B. Stefanovich, "Degradation and breakdown in anodic tantalum oxide," *Izvestiya Vysshikh Uchebnykh Zavedenii, Fizika*, vol. 5, pp. 15-19, 1984.
- [6] J.-P. Manceau, S. Bruyerel, S. Jeannot, A. Sylvestre, and P. Gonon, "Leakage current variation with time in Ta<sub>2</sub>O<sub>5</sub> MIM and MIS capacitors," in *IEEE International Integrated Reliability Workshop*, 2006, pp. 129-133.
- [7] J.-P. Manceau, S. Bruyère, S. Jeannot, A. Sylvestre, and P. Gonon, "Current Instability, Permittivity Variation With Frequency, and Their Relationship in Ta<sub>2</sub>O<sub>5</sub> Capacitor," *IEEE TRANSACTIONS ON DEVICE AND MATERIALS RELIABILITY*, vol. 7, pp. 315-323, 2007.
- [8] Y. Freeman, R. Hahn, P. Lessner, and J. Prymak, "Reliability and Critical Applications of Tantalum Capacitors," presented at CARTS Europe, Barcelona, Spain, 2007.
- [9] E. K. Reed, "Tantalum chip capacitor reliability in high surge and ripple current applications," presented at 44th. Electronic Components and Technology Conference, 1994.
- [10] S. Zednicek, I. Horacek, J. Petrzilek, P. Jacisko, P. Gregorova, and T. Zednicek, "High CV Tantalum Capacitors – Challenges and Limitations," presented at CARTS Europe, Helsinki, Finland, 2008.
- [11] T. Zednicek, J. Sikula, and H. Leibovitz, "A Study of Field Crystallization in Tantalum Capacitors and its effect on DCL and Reliability," in *29th symposium for passive components, CARTS'09*. Jacksonville, FL, 2009, pp. 5.3.1-11.
- [12] R. Chen, "On the analysis of thermally stimulated processes," in *Thermally stimulated processes in solids: new prospects*, J.P. Fillard and J. v. Turnhout, Eds. Amsterdam, Oxford, New York: Elsevier scientific publishing company, 1977, pp. 15-24.
- [13] G. P. Klein and N. I. Jaeger, "Electron injection into anodic tantalum oxide assisted by ionic interface polarization," *Journal of the Electrochemical Society*, vol. 117, pp. 1483-1494, 1970.
- [14] G. P. Klein and N. I. Jaeger, "Electron injection into anodic valve metal oxides," *Journal of the Electrochemical Society*, vol. 119, pp. 1531-1538, 1972.
- [15] L. Badian, S. M. Gubanski, and T. J. Lewis, "Anomalous conduction and ageing effects in rutile (TiO<sub>2</sub>) ceramics," *J. Phys. D: Appl. Phys.*, vol. 10, pp. 2513-2523, 1977.

- [16] M. Hayashi, M. Haba, S. Hirano, M. Okamoto, and M. Watanabe, "Degradation Mechanism of Zinc-Oxide Varistors under Dc Bias," *Journal of Applied Physics*, vol. 53, pp. 5754-5762, 1982.
- [17] Z. Yuanxiang and N. Yoshimura, "An investigation on DC conduction in ceramic capacitors," in *International Symposium on Electrical Insulating Materials*. Toyohashi, Japan, 1998, pp. 123-126.
- [18] F. Chiu, J. Wang, J. Lee, and S. Wu, "Leakage currents in amorphous Ta<sub>2</sub>O<sub>5</sub> thin films," *Journal of Applied Physics*, vol. 81, pp. 6911-6915, 1997.
- [19] C. Chaneliere, J. Autran, R. Devine, and B. Balland, "Tantalum pentoxide (Ta<sub>2</sub>O<sub>5</sub>) thin films for advanced dielectric applications," *Material Science and Engineering*, vol. R22, pp. 269-322, 1998.
- [20] E. Atanassova and A. Paskaleva, "Conduction mechanisms and reliability of thermal Ta<sub>2</sub>O<sub>5</sub>-Si structures and the effect of the gate electrode," *Journal of Applied Physics*, vol. 97, pp. 1-11, 2005.
- [21] J. C. Schug, A. C. Lilly, and D. A. Lowitz, "Schottky Currents in Dielectric Films," *Physical Review B*, vol. 1, pp. 4811-4818, 1970.
- [22] J. S. Lee, S. J. Chang, J. F. Chena, S. C. Sunb, C. H. Liuc, and U. H. Liawd, "Effects of O<sub>2</sub> thermal annealing on the properties of CVD Ta<sub>2</sub>O<sub>5</sub> thin films," *Materials Chemistry and Physics*, vol. 77, pp. 242-247, 2002.
- [23] N. Novkovski and E. Atanassova, "A comprehensive model for the I-V characteristics of metal-Ta<sub>2</sub>O<sub>5</sub>/SiO<sub>2</sub>-Si structures," *Applied Physics a-Materials Science & Processing*, vol. 83, pp. 435-445, 2006.
- [24] J. Pavelka, J. Sikula, P. Vasina, V. Sedlakova, M. Tacano, and S. Hashiguchi, "Noise and transport characterisation of tantalum capacitors," *Microelectronics Reliability*, vol. 42, pp. 841-847, 2002.
- [25] R. M. Fleming, D. V. Lang, and C. D. Jones, "Defect dominated charge transport in amorphous Ta<sub>2</sub>O<sub>5</sub> thin films," *Journal of Applied Physics*, vol. 88, pp. 850-862, 2000.
- [26] D. Spassov, E. Atanassova, and D. Virovska, "Electrical characteristics of Ta<sub>2</sub>O<sub>5</sub> based capacitors with different gate electrodes," *Applied Physics a-Materials Science & Processing*, vol. 82, pp. 55-62, 2006.
- [27] Y. Freeman, W. R. Harrell, I. Luzinov, B. Holman, and P. Lessner, "Electrical Characterization of Tantalum Capacitors with Poly(3,4-ethylenedioxythiophene) Counter Electrodes," *Journal of the Electrochemical Society*, vol. 156, pp. G65-G70, 2009.
- [28] F. C. Aris and T. J. Lewis, "Steady and Transient Conduction Processes in Anodic Tantalum Oxide," *Journal of Physics D-Applied Physics*, vol. 6, pp. 1067-1083, 1973.
- [29] S. Zafar, R. E. Jones, B. Jiang, B. White, P. Chu, D. Taylor, and S. Gillespie, "Oxygen vacancy mobility determined from current measurements in thin Ba<sub>0.5</sub>Sr<sub>0.5</sub>TiO<sub>3</sub> films," *Applied Physics Letters*, vol. 73, pp. 175-177, 1998.
- [30] W. Liu and C. A. Randall, "Thermally Stimulated Relaxation in Fe-Doped SrTiO<sub>3</sub> Systems: II. Degradation of SrTiO<sub>3</sub> Dielectrics," *Journal of the American Ceramic Society*, vol. 91, pp. 3251-3257, 2008.
- [31] W. S. Lau, L. L. Leong, T. J. Han, and N. P. Sandler, "Detection of oxygen vacancy defect states in capacitors with ultrathin Ta<sub>2</sub>O<sub>5</sub> films by zero-bias thermally stimulated current spectroscopy," *Applied Physics Letters*, vol. 83, pp. 2835-2837, 2003.
- [32] W. S. Lau, "Similarity between the first ionized state of the oxygen vacancy double donor in tantalum oxide and the first ionized state of the cadmium vacancy double acceptor in cadmium sulfide," *Applied Physics Letters*, vol. 90, 2007.
- [33] H. Sawada and K. Kawakami, "Electronic structure of oxygen vacancy in Ta<sub>2</sub>O<sub>5</sub>," *Journal of Applied Physics*, vol. 86, pp. 956-959, 1999.
- [34] W. S. Lau, T. S. Tan, and P. Babu, "Mechanism of leakage current reduction of tantalum oxide capacitors by titanium doping," *Applied Physics Letters*, vol. 90, 2007.